

Biodegradable and plasma-treated electrospun scaffolds coated with recombinant Olfactomedin-like 3 for accelerating wound healing and tissue regeneration

Louise L. Dunn, PhD¹; Sarra de Valence, PhD²; Jean-Christophe Tille, MD, PhD³; Philippe Hammel⁴; Beat H. Walpoth² MD PhD; Roland Stocker¹ PhD; Beat A. Imhof⁴ PhD; Marijana Miljkovic-Licina, PhD⁴

1. *Vascular Biology Division, Victor Chang Cardiac Research Institute, and School of Medical Sciences, University of New South Wales, Sydney, Australia*

2. *Service of Cardiovascular Surgery, Geneva University Hospital, Geneva, Switzerland*

3. *Division of Clinical Pathology, Geneva University Hospital, Geneva, Switzerland*

4. *Department of Pathology and Immunology, University of Geneva Medical Center, Geneva, Switzerland*

Reprints requests:

Marijana Miljkovic-Licina, PhD, Department of Pathology and Immunology, University of Geneva Medical Center, rue Michel-Servet 1, CH-1211 Geneva 4, Switzerland.

Tel: +41 22 37 957 56;

Fax: +41 22 379 57 46;

Email: marijana.licina@unige.ch

Short running title: Matricellular protein Olfactomedin-like 3 promotes neovascularization

Key words: Olfactomedin-like 3, electrospun scaffold, neovascularization, wound healing, tissue remodeling

COPYRIGHT STATEMENT. This is the author's version of a work that was accepted for publication. Changes introduced as a result of publishing processes such as copy-editing and formatting may not be reflected in this work. For a definitive version of this work please refer to the published source.

This is the peer reviewed author's version of the following article: Dunn, Louise L and de Valence, Sarra and Tille, Jean-Christophe and Hammel, Philippe and Walpoth, Beat H and Stocker, Roland and Imhof, Beat A and Miljkovic-Licina, Marijana (2016) Biodegradable and plasma-treated electrospun scaffolds coated with recombinant Olfactomedin-like 3 for accelerating wound healing and tissue regeneration. *Wound Repair and Regeneration*, 24 (6). pp.1030-1035 Final publication is available from <http://dx.doi.org/10.1111/wrr.12485>

This article may be used for non-commercial purposes in accordance with the Creative Commons Attribution-NonCommercial- NoDerivatives 4.0 International licence <http://creativecommons.org/licenses/by-nc-nd/4.0/>

This article has been accepted for publication and undergone full peer review but has not been through the copyediting, typesetting, pagination and proofreading process which may lead to differences between this version and the Version of Record. Please cite this article as an 'Accepted Article', doi: 10.1111/wrr.12485

ABSTRACT (150 words)

Three-dimensional biomimetic scaffolds resembling the native extracellular matrix (ECM) are widely used in tissue engineering, however they often lack optimal bioactive cues needed for acceleration of cell proliferation, neovascularization and tissue regeneration. In this study, the use of the ECM-related protein Olfactomedin-like 3 (Olfml3) demonstrates the importance and feasibility of fabricating efficient bioactive scaffolds without *in vitro* cell seeding prior to *in vivo* implantation. First, *in vivo* proangiogenic properties of Olfml3 were shown in a murine wound healing model by accelerated wound closure and a 1.4-fold increase in wound vascularity. Second, subcutaneous implantation of tubular scaffolds coated with recombinant Olfml3 resulted in enhanced cell in-growth and neovascularization compared with control scaffolds. Together, our data indicates the potential of Olfml3 to accelerate neovascularization during tissue regeneration by promoting endothelial cell proliferation and migration. This study provides a promising concept for the reconstruction of damaged tissue using affordable and effective bioactive scaffolds.

Body text (1500 words)

Extra-cellular matrix (ECM) acts as a scaffold providing major cues that direct cell attachment, alignment, proliferation, migration, and proper physiological functions of various tissues. It also sequesters growth factors and plays a role in tissue growth, remodeling and regeneration.¹ Tissue injuries and defects are often repaired using alternative graft materials like tissue substitutes that serve as scaffolds for host cells and support tissue remodeling.² A challenge for the future of tissue engineering is the creation of alternatives of tissue grafts that mimic native structures, and facilitate wound healing and regeneration. Engineered substitutes are composed either of synthetic polymers, natural ECM-derived materials or a combination of these.³ In particular, electrospun polymer scaffolds have substantial potential for tissue engineering due to their high surface to volume ratio and the characteristics of their nanofibers with interconnected pores that facilitate transport of nutrients and waste removal, hence mimicking native ECM.⁴ Recent studies combined natural and synthetic molecules to generate scaffolds with both cell instructive biochemical cues and favorable mechanical characteristics.⁵ Furthermore, pre-seeding cells on a scaffold prior to *in vivo* implantation to bypass the ECM remodeling process promotes greater wound healing and tissue regeneration than acellular scaffolds.⁶ Unfortunately, this approach is time-consuming and costly. Therefore, there is an unmet clinical need for tissue regenerative scaffolds with high bioactivity rates resembling autologous tissue or with higher efficiency and cost-effectiveness in terms of manufacturing.

The main goal of this study was to develop biomimetic scaffolds releasing growth factors or other bioactive molecules that lead to the desired cell response and enhance tissue remodeling without the need for *in vitro* cell seeding prior to the *in vivo* implantation. We previously described Olfactomedin-like 3 (Olfml3), an ECM protein with proangiogenic properties that

regulates vascular remodeling under normal and pathological conditions.⁷ Olfml3 serves as a scaffold protein that recruits bone morphogenetic protein 1 (BMP1) to its substrate chordin, a BMP antagonist.⁸ We demonstrated that both mouse and human Olfml3 proteins interact with BMP4, a potent proangiogenic factor. Olfml3 alone or through binding to BMP4 enhances the canonical SMAD1/5/8 signaling pathway required for BMP4-induced endothelial cell activation.⁷ Here, we explored the *in vivo* benefits of Olfml3 in promoting neovascularization in a mouse wound healing model and in tissue remodeling after subcutaneous injection of electrospun polymer scaffolds in rats.

We first proceeded to determine the role of Olfml3 in physiological neovascularization using a murine wound healing model. In this model, full thickness cutaneous wounds are created.

The wounds are splinted to prevent contraction and encourage granulation tissue formation, re-epithelialization, and neovascularization. We observed that topical application of murine recombinant Olfml3-FLAG-tagged protein to the wound bed for 6 days resulted in significant acceleration of wound closure compared to PBS-treated control wounds, as determined using a caliper-based macroscopic method (Figure 1A). This observation was supported by histological assessment of wound width on hematoxylin and eosin-stained tissue sections (Figure 1B). Accelerated wound closure was associated with a 1.4 ± 0.1 -fold increase in wound vascularity at day 6 post-wounding, as assessed by the area of CD31-positive vessels in the wound bed of recombinant Olfml3-FLAG-tagged treated wounds compared to PBS-treated control wounds (Figure 1C). Double immunostaining of wounds for Olfml3 and CD31 revealed that Olfml3 protein was enriched in the epidermal cells and in the endothelial cells of a subset of CD31-positive epidermal and dermal vessels of recombinant Olfml3-FLAG-tagged treated wounds compared to PBS-treated control wounds (Figure 1D). In addition, Olfml3 protein was expressed by a small subset of mononuclear phagocytic cells, as assessed by double staining of wounds for F4-80 and Olfml3 (Figure 1E). In a subset of mice,

recombinant Olfml3-FLAG-tagged protein was applied for 10 days, by which time the wounds had closed. At this time point, no significant differences in wound vascularity were apparent (data not shown). This is consistent with the remodeling phase that occurs following wound closure. Taken together, these data indicate that Olfml3 has proangiogenic action that accelerates wound closure during wound healing via enhanced migration and attachment of host endothelial cells in the course of tissue remodeling.

Polycaprolactone (PCL) is a biodegradable synthetic polymer with favorable mechanical properties, which has been approved by the FDA for certain clinical applications.⁹ Our prior studies focused on developing cardiovascular regenerative PCL scaffolds with optimal pore diameters for cell migration and infiltration.¹⁰ Having positive experiences with electrospun PCL implants in subcutaneous and vascular locations such as the rat abdominal aorta or the porcine carotid artery,^{11, 12} we decided to investigate the potential beneficial effect of adding recombinant murine Olfml3-FLAG-tagged protein to the electrospun PCL in an *in vivo* subcutaneous model. Electrospun PCL scaffolds were prepared and cut as patches for *in vitro* analysis or tubular grafts for *in vivo* implantations. A detailed description of the fiber and pore size as well as total porosity of these grafts has been previously described.¹⁰ Patches and tubular grafts were then treated by air plasma for 30 sec, as described elsewhere¹³ and in the Supplementary data file. Gas plasma treatment is known to improve the hydrophilicity of PCL polymer surfaces and to form functional groups that serve for the attachment of peptides, drugs or native polymers.¹⁴ Standard (untreated) and plasma-treated patches were then coated with increasing concentrations of recombinant murine Olfml3-FLAG-tagged protein (0-1 $\mu\text{g/mL}$) and the amount of bound protein onto the patches was measured using an HRP-labeled anti-Olfml3 antibody (Figure 2A, upper panel). Due to plasma treatment, recombinant Olfml3-FLAG-tagged protein bound to plasma-treated PCL patches with a higher affinity compared to standard (untreated) patches (Figure 2A, lower panel),

confirming our previous finding of increased hydrophilicity and bioavailability of plasma-treated PCL scaffolds.¹³ Next, the tubular grafts (inner diameter: 2 mm, length: 1 cm) were treated by plasma for 30 sec and then coated with 1 μ g/mL recombinant Olfml3-FLAG-tagged protein or PBS (control) before being evaluated in rats (Figure 2B). Grafts were implanted subcutaneously on both dorsal and ventral sides of the animals for a 21-day period (Figure 2B, upper panels). The rats were then sacrificed and the implants and their surrounding tissue were retrieved. After 21 days of subcutaneous implantation, dense cell infiltration from the outer side of recombinant Olfml3 FLAG-tagged protein treated or control grafts was observed. The lumen of the implants towards the center of the tubes was still void of tissue, resulting in cell infiltration only from the outer side (Figure 2B, middle panels, arrows). At the interface between the tissue and the grafts, no major inflammatory reaction was observed, and no thick fibrous capsule formed around the implants (Figure 2B, middle panels, arrowheads). Of interest, the infiltrate had a significantly higher cell density in plasma-treated grafts coated with recombinant Olfml3-FLAG-tagged protein compared to the PBS-coated controls (Figure 2B, lower panels and Figure 2C). Furthermore, cell infiltrations were mainly composed of fibroblasts, monocytes/macrophages, and endothelial cells, as assessed by immunostaining of implants for β -actin and F4-80, and CD31 and Olfml3, respectively (Figure 2D). Cellular infiltration of PCL grafts coated with recombinant Olfml3-FLAG-tagged protein was accompanied by moderate neovascularization reaching the three-quarter thickness of the implant, while control group showed only a scarce number of superficially penetrating endothelial cells, as confirmed by CD34 immunostainings (Figure 2E and 2F,). These results confirmed that the plasma-treated electrospun PCL scaffolds could provide an optimal environment for cellular repopulation, while Olfml3 coating may enhance migration and attachment of host endothelial cells in the course of tissue remodeling.

Combining biodegradable synthetic polymers with growth factors may improve their bioactivity and enhance cell attachment, proliferation and angiogenesis and therefore, facilitate tissue regeneration.¹⁵ In this study, we showed that the combination of nanotopography, plasma treatment and coating of electrospun PCL scaffolds with the proangiogenic protein Olfm13 accelerated cell in-growth, migration and neovascularization in a subcutaneous implantation rat model over a 21-day period. Furthermore, Olfm13 enhanced wound closure and neovascularization at early time points in a mouse wound healing model, thus accelerating the process of tissue regeneration. Taken together, our study suggests that the plasma-treated electrospun PCL scaffolds combined with a proangiogenic Olfm13 protein, is a prototype of a simple, effective and affordable substitute for tissue regeneration where cell pre-seeding and proliferation prior to the *in vivo* implantation is not an option.

Acknowledgements

The authors would like to acknowledge the assistance of Antoine Poncet in the statistical data analysis. MML and BAI acknowledge support from the Swiss National Science Foundation (FNS 310030-153456) and the Clayton Foundation for Research (ME7202-102028). RS acknowledges support from the National Health and Medical Research Council of Australia, including Senior Principal Research Fellowships 1003484 and 1111632.

Conflicts of Interest: No financial interests or conflicts of interest exist for any of the authors.

References

1. Schultz GS, Wysocki A. Interactions between extracellular matrix and growth factors in wound healing. *Wound Repair Regen* 2009;17: 153-162.
2. Jayarama Reddy V, Radhakrishnan S, Ravichandran R, Mukherjee S, Balamurugan R, Sundarrajan S, et al. Nanofibrous structured biomimetic strategies for skin tissue regeneration. *Wound Repair Regen* 2013;21: 1-16.
3. Thottappillil N, Nair PD. Scaffolds in vascular regeneration: current status. *Vasc Health Risk Manag* 2015;11: 79-91.
4. Hassiba AJ, El Zowalaty ME, Nasrallah GK, Webster TJ, Luyt AS, Abdullah AM, et al. Review of recent research on biomedical applications of electrospun polymer nanofibers for improved wound healing. *Nanomedicine (Lond)* 2016;11: 715-737.
5. Kim BR, Nguyen TB, Min YK, Lee BT. In vitro and in vivo studies of BMP-2-loaded PCL-gelatin-BCP electrospun scaffolds. *Tissue Eng Part A* 2014;20: 3279-3289.
6. Bonvallet PP, Schultz MJ, Mitchell EH, Bain JL, Culpepper BK, Thomas SJ, et al. Microporous dermal-mimetic electrospun scaffolds pre-seeded with fibroblasts promote tissue regeneration in full-thickness skin wounds. *PLoS One* 2015;10: e0122359.
7. Miljkovic-Licina M, Hammel P, Garrido-Urbani S, Lee BP, Meguenani M, Chaabane C, et al. Targeting Olfactomedin-like 3 inhibits tumor growth by impairing angiogenesis and pericyte coverage. *Mol Cancer Ther* 2012;11: 2588-2599.
8. Inomata H, Haraguchi T, Sasai Y. Robust stability of the embryonic axial pattern requires a secreted scaffold for chordin degradation. *Cell* 2008;134: 854-865.
9. Mogosanu GD, Grumezescu AM. Natural and synthetic polymers for wounds and burns dressing. *Int J Pharm* 2014;463: 127-136.

10. de Valence S, Tille JC, Giliberto JP, Mrowczynski W, Gurny R, Walpoth BH, et al. Advantages of bilayered vascular grafts for surgical applicability and tissue regeneration. *Acta Biomater* 2012;8: 3914-3920.
11. de Valence S, Tille JC, Mugnai D, Mrowczynski W, Gurny R, Moller M, et al. Long term performance of polycaprolactone vascular grafts in a rat abdominal aorta replacement model. *Biomaterials* 2011;33: 38-47.
12. Mrowczynski W, Mugnai D, de Valence S, Tille JC, Khabiri E, Cikirikcioglu M, et al. Porcine carotid artery replacement with biodegradable electrospun poly-ε-caprolactone vascular prosthesis. *J Vasc Surg* 2014;59: 210-219.
13. de Valence S, Tille JC, Chaabane C, Gurny R, Bochaton-Piallat ML, Walpoth BH, et al. Plasma treatment for improving cell biocompatibility of a biodegradable polymer scaffold for vascular graft applications. *Eur J Pharm Biopharm* 2013;85: 78-86.
14. Kim HS, Yoo HS. Therapeutic application of electrospun nanofibrous meshes. *Nanomedicine (Lond)* 2014;9: 517-533.
15. Zhang H, Jia X, Han F, Zhao J, Zhao Y, Fan Y, et al. Dual-delivery of VEGF and PDGF by double-layered electrospun membranes for blood vessel regeneration. *Biomaterials* 2013;34: 2202-2212.

Figure Legends

Figure 1. Effect of Olfml3 on wound healing and neovascularization in mouse wound healing model. Female C57BL/6JArc mice (8-9 week old, n=10) had two 5 mm diameter full thickness excisional cutaneous wounds surgically introduced. Wounds were measured using calipers before recombinant Olfml3-FLAG-tagged protein (10 μ g in 50 μ L PBS, right wound) or vehicle control (left wound) was applied to the wounds daily for six days. (A) Recombinant Olfml3-FLAG-tagged protein accelerated wound closure as determined using calipers. Ruler gradations on photomicrographs = 1 mm. (B) Hematoxylin and eosin stained section demonstrating decreased wound width in recombinant Olfml3-FLAG-tagged treated wounds. Photomicrographs at 1.6x magnification, white scale bar = 2 mm, black line indicates wound width. (C) Recombinant Olfml3-FLAG-tagged protein increased wound bed vascularity as determined by the total fluorescent area of CD31-phycoerythrin positive vessels (CD31, arrows). Isotype IgG2 κ -phycoerythrin control is shown. Bright-field (BF) and fluorescent photomicrographs (CD31) are shown in parallel. Photomicrographs at 20x magnification, scale bar = 100 μ m. Results are expressed as mean \pm SD. (D) Olfml3 protein distribution in the epidermal cells (arrowheads) and endothelial cells of a subset of CD31-positive epidermal and dermal vessels (arrows) of recombinant Olfml3-FLAG-tagged treated wounds compared to PBS-treated control wounds. Bright-field (BF) and fluorescent photomicrographs (Olfml3+CD31, overlay) are shown in parallel. Photomicrographs at 40x magnification, scale bar = 50 μ m. (E) Cell populations reacting to and infiltrating wounds treated with either control (E, control) or recombinant Olfml3-FLAG-tagged protein (rOlfml3-FLAG): endothelial cells (Olfml3, green, arrows) and monocytes/macrophages (F4-80, red, arrowheads), as assessed by immunostaining of wounds for Olfml3 and F4-80. Bright-field (BF) and fluorescent photomicrographs (Olfml3+F4-80, overlay) are shown in

parallel. Photomicrographs at 40x magnification, scale bar = 50 μm . Results in (A) were analyzed by Repeated Measures 2-way ANOVA with Sidak's Multiple Comparison test, with results in (C) analyzed by the Mann Whitney test (Prism version 6.0c software). * $p < 0.05$ compared to PBS control.

Figure 2. Olfml3-coated biodegradable electrospun scaffolds for *in vivo* tissue graft development. Electrospun PCL scaffolds were prepared and cut to make either patches with an average thickness of 260 ± 47 μm for surface coating (A) or 1 cm long tubular grafts with an average thickness of 598 ± 39 μm and a 2 mm inner diameter for *in vivo* implantations (B-F). (A) Coating of control and plasma-treated patches with increasing concentrations of recombinant Olfml3-FLAG-tagged protein (0-1 $\mu\text{g/mL}$). An HRP-labeled anti-Olfml3 antibody measured the amount of bound protein onto the patches (three samples per group; two independent experiments). (B) Histological cross-sections of tubular scaffolds coated with either PBS (B, control, left) or 1 $\mu\text{g/mL}$ recombinant Olfml3-FLAG-tagged (B, rOlfml3-FLAG, right) and implanted subcutaneously on dorsal or ventral sides of male Sprague-Dawley rats ($n=3$) and kept for 21 days, as follows: macroscopical view (B, upper panels) and magnified views with cellular infiltrations stained by the hematoxylin and eosin method (B, lower panels). Photomicrographs at 5x and 40x magnification, scale bar = 1 mm and 100 μm , respectively. (C) Quantification of cell density in the outside edge of the grafts. Results are expressed as mean \pm SD. (D) Cell populations reacting to and infiltrating subcutaneous tubular scaffolds coated with either control (D, control) or recombinant Olfml3-FLAG-tagged protein (D, rOlfml3-FLAG): monocytes/macrophages (D, F4-80, red); fibroblasts (D, β -actin, green); and endothelial cells (D, Olfml3, red and CD31, green); as assessed by immunostaining of implants for respective molecular markers. Photomicrographs at 40x magnification, scale bar = 100 μm . (E, F) Recombinant Olfml3-FLAG-tagged protein increased neovascularization as determined by the number of CD34-positive vessels.

Photomicrographs at 20x and 40x magnification, scale bar = 50 μm and 100 μm , respectively.

Results are expressed as mean \pm SD. Results in (C and F) were analyzed by the Mann Whitney test (Prism version 6.0 software). * $p < 0.05$ compared to control.

Accepted Article

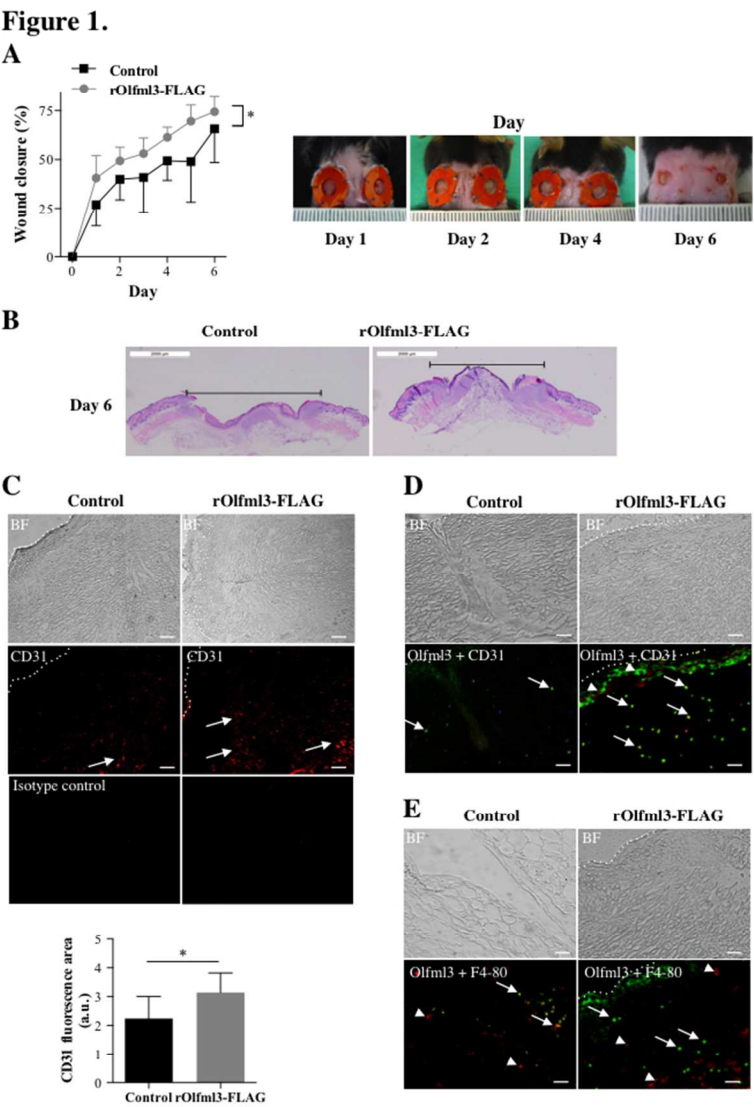


Figure 1. Effect of Olfml3 on wound healing and neovascularization in mouse wound healing model. Female C57BL/6JArc mice (8-9 week old, n=10) had two 5 mm diameter full thickness excisional cutaneous wounds surgically introduced. Wounds were measured using calipers before recombinant Olfml3-FLAG-tagged protein (10 μ g in 50 μ L PBS, right wound) or vehicle control (left wound) was applied to the wounds daily for six days. (A) Recombinant Olfml3-FLAG-tagged protein accelerated wound closure as determined using calipers. Ruler gradations on photomicrographs = 1 mm. (B) Hematoxylin and eosin stained section demonstrating decreased wound width in recombinant Olfml3-FLAG-tagged treated wounds. Photomicrographs at 1.6x magnification, white scale bar = 2 mm, black line indicates wound width. (C) Recombinant Olfml3-FLAG-tagged protein increased wound bed vascularity as determined by the total fluorescent area of CD31-phycoerythrin positive vessels (CD31, arrows). Isotype IgG2ak-phycoerythrin control is shown. Bright-field (BF) and fluorescent photomicrographs (CD31) are shown in parallel. Photomicrographs at 20x magnification, scale bar = 100 μ m. Results are expressed as mean \pm SD. (D) Olfml3 protein distribution in the epidermal cells (arrows) and endothelial cells of a subset of CD31-

positive epidermal and dermal vessels (arrows) of recombinant Olfml3-FLAG-tagged treated wounds compared to PBS-treated control wounds. Bright-field (BF) and fluorescent photomicrographs (Olfml3+CD31, overlay) are shown in parallel. Photomicrographs at 40x magnification, scale bar = 50 μ m. (E) Cell populations reacting to and infiltrating wounds treated with either control (E, control) or recombinant Olfml3-FLAG-tagged protein (rOlfml3-FLAG): endothelial cells (Olfml3, green, arrows) and monocytes/macrophages (F4-80, red, arrowheads), as assessed by immunostaining of wounds for Olfml3 and F4-80. Bright-field (BF) and fluorescent photomicrographs (Olfml3+F4-80, overlay) are shown in parallel. Photomicrographs at 40x magnification, scale bar = 50 μ m. Results in (A) were analyzed by Repeated Measures 2-way ANOVA with Sidak's Multiple Comparison test, with results in (C) analyzed by the Mann Whitney test (Prism version 6.0c software). * $p < 0.05$ compared to PBS control.

254x366mm (72 x 72 DPI)

Figure 2.

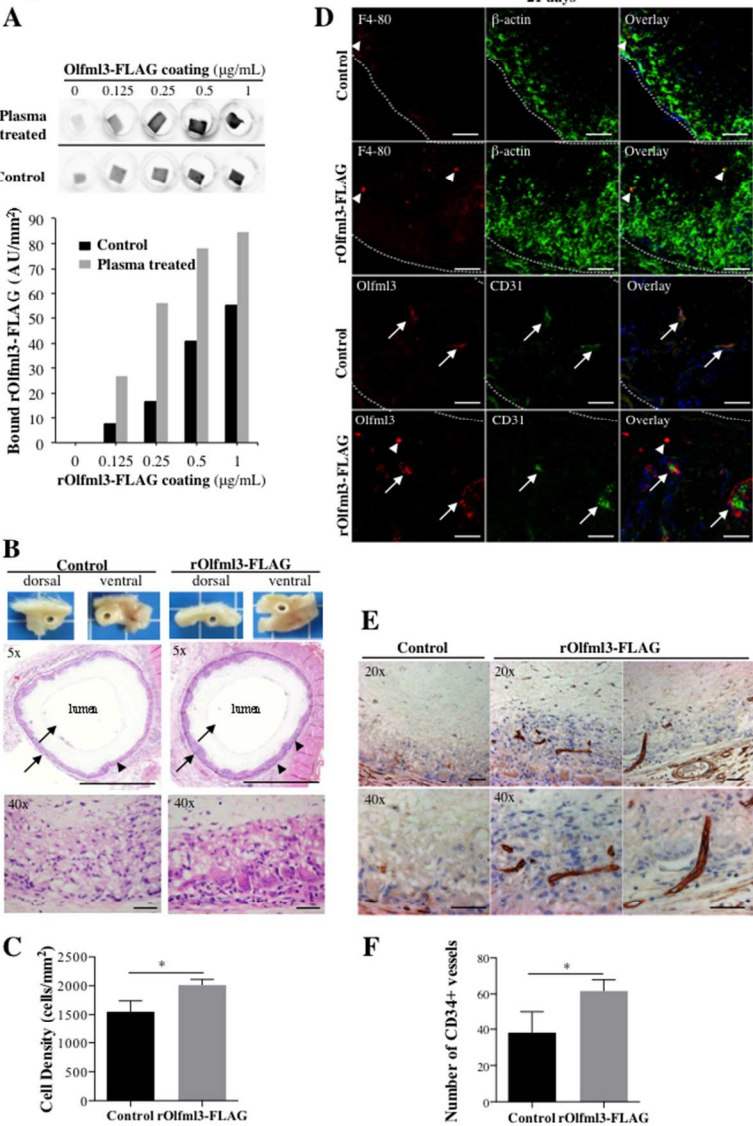


Figure 2. Olfml3-coated biodegradable electrospun scaffolds for in vivo tissue graft development. Electrospun PCL scaffolds were prepared and cut to make either patches with an average thickness of $260\pm47\ \mu\text{m}$ for surface coating (A) or 1 cm long tubular grafts with an average thickness of $598\pm39\ \mu\text{m}$ and a 2 mm inner diameter for in vivo implantations (B-F). (A) Coating of control and plasma-treated patches with increasing concentrations of recombinant Olfml3-FLAG-tagged protein (0-1 $\mu\text{g/mL}$). An HRP-labeled anti-Olfml3 antibody measured the amount of bound protein onto the patches (three samples per group; two independent experiments). (A, upper and middle panel). Long-term stability of recombinant Olfml3-FLAG binding on plasma-treated PCL patches measured over a period of 21-days (A, lower panel). (B) Histological cross-sections of tubular scaffolds coated with either PBS (B, control, left) or 1 $\mu\text{g/mL}$ recombinant Olfml3-FLAG-tagged (B, rOlfml3-FLAG, right) and implanted subcutaneously on dorsal or ventral sides of male Sprague-Dawley rats ($n=3$) and kept for 21 days, as follows: macroscopical view (B, upper panels) and magnified views with cellular infiltrations stained by the hematoxylin and eosin method (B, lower panels). Photomicrographs at 5x and 40x magnification, scale bar = 1 mm and 100 μm ,

respectively. (C) Quantification of cell density in the outside edge of the grafts. Results are expressed as mean \pm SD. (D) Cell populations reacting to and infiltrating subcutaneous tubular scaffolds coated with either control (D, control) or recombinant Olfml3-FLAG-tagged protein (D, rOlfml3-FLAG):

monocytes/macrophages (D, F4-80, red); fibroblasts (D, β -actin, green); and endothelial cells (D, Olfml3, red and CD31, green); as assessed by immunostaining of implants for respective molecular markers.

Photomicrographs at 40x magnification, scale bar = 100 μ m. (E, F) Recombinant Olfml3-FLAG-tagged protein increased neovascularization as determined by the number of CD34-positive vessels.

Photomicrographs at 20x and 40x magnification, scale bar = 50 μ m and 100 μ m, respectively. Results are expressed as mean \pm SD. Results in (C and F) were analyzed by the Mann Whitney test (Prism version 6.0 software). * $p < 0.05$ compared to control.

254x366mm (72 x 72 DPI)